

## A Model Predictive Compensator Strategy for Performance Improvement of Hybrid Energy Storage Systems in DC Microgrids

S. RUBEENA BI<sup>1</sup>, M.SWATHI<sup>2</sup>, S.UME SALMA<sup>3</sup>, K.UMA MANASA<sup>4</sup>, K.VAMSI KRISHNA<sup>5</sup>, K.UDAY KUMAR<sup>6</sup>

<sup>1,2</sup>Assistant professor, Department of Electrical and Electronics Engineering, Annamacharya Institute of Technology and Sciences (AITS), Rajampet.

<sup>3,4,5,6</sup>Student of Electrical Engineering, Annamacharya Institute of Technology and Sciences (AITS), Rajampet..

**ABSTRACT:** The most typical method used in DC microgrid (MG) applications for battery-supercapacitor Hybrid Energy Storage Systems (HESSs) is Filtration-Based (FB) power/current allocation. In this method, the input power/current of the HESS is divided into high-frequency and low-frequency components, and the high-frequency components are subsequently assigned to the SC. Additionally, this strategy necessitates a rule-based supervisory controller, which may cause SC to stop functioning, in order to prevent the State of Charge violation (SoC) of SC. In order to study the effects of an FB current allocation system on the dynamic stability of an islanded DC MG in which a grid-forming HESS supplies a Constant Power Load (CPL), this paper first presents a small-signal stability analysis. Then, it demonstrates that the ongoing operation if the grid-forming HESS is loaded by huge CPLs, of SC is crucial. In order to solve this problem, this research suggests a Model Predictive Control (MPC) method that collaborates with a high-pass filter to carry out the battery and SC current assignment. This method ensures the ongoing operation of SC by automatically restoring the SoC of SC after abrupt load changes and limiting its SoC variation in a pre-set range. Indirectly enabling the MG's Proportional-Integral (PI) voltage controller to work with larger gain values, which improves transient response and voltage quality, is the goal of the suggested FB-MPC technique. The system is then simulated in MATLAB/Simulink to validate the performance of the suggested approach.

**Index-Terms-**Filtration-based power/current allocation systems, battery/supercapacitor hybrid energy storage systems, model predictive control, stability analysis, state of charge recovery.

### NOMENCLATURE

#### A. ABBREVIATIONS

BESS	Battery Energy Storage System.
CPL	Constant Power Load.
CPS	Constant Power Source.
DC	Direct Current.
DER	Distributed Energy Resources.
FB	Filtration Based.
HESS	Hybrid Energy Storage System.
HPF	High Pass Filter.
LTI	Linear Time Invariant.
EMS	Energy management system.
MG	Micro Grid.
MPC	Model Predictive Control.
MPPT	Maximum Power Point Tracking.
PPL	Pulsed Power Load.
PV	Photo Voltaic.
SC	Super Capacitor.
SoC	State of Charge.

#### B. SYMBOLS

$d_1$	Duty cycle of the BESS converter.
$d_2$	Duty cycle of the SC converter.
$d_{com}$	Compensation term added/subtracted to/from the SC/BESS reference current.
$i_{CP}$	Resultant current of the CPL and CPS.
$i_{com}$	MPC compensation current.
$i_{HESS}$	HESS output current.
$i_{HPF}$	Output current of the high-pass filter.
$i_{L1}$	Inductor current of the BESS.
$i_{L2}$	Inductor current of the SC.
$i_{Load}$	Load Current.
$i_{PV}$	PV output current.
$i_{ref}$	Reference current of the HESS computed by the voltage controller.
$SoC_{max}$	Maximum allowable SoC for SC.
$SoC_{min}$	Minimum allowable SoC for SC.
$SoC_{ref}$	Reference SoC of the SC.
$SoC_{SC}$	SoC of the SC.
$v_b$	Terminal voltage of the BESS.
$v_{ref}$	Reference voltage of the voltage controller
$v_{SC}$	Terminal voltage of SC.

### I. INTRODUCTION

#### A. LITERATURE REVIEW

Micro Grids (MGs) are autonomous active distribution networks that can improve the performance of conventional power grids by boosting customer engagement, penetration of renewable energy sources, stability of the power grid, and grid resilience [1], [2]. Because they have less control complexity and fewer power conversion losses than AC MGs, DC MGs have recently attracted a lot of attention. DC MGs can be viewed as workable options for improving the resilience of power systems, electrifying rural areas, and assisting local energy communities [3]. The existence of Continuous Power Loads (CPLs) and Pulsed Power Loads (PPLs), which call for a quick dynamic reaction and a substantial stability margin of the control system [4]-[6], might make controlling DC MGs difficult. Highly-dispatchable Distributed Energy Resources (DERs) as well as other technologies can be used to increase the system's transient response, stability, and flexibility, improved control and management methods are needed [7].

One of the most common energy storage sources for MG applications are Battery Energy Storage Systems (BESSs). BESSs have low energy losses, are dispatchable, and are very inexpensive. Additionally, they are well suited for peak shaving and steady-state power balancing due to their high energy density [8], [9]. Due to their low power density, the BESSs may, however, exhibit very poor transient response during rapid load changes [7], [10]. As a result, in the presence of PPLs, grid-forming BESSs may not deliver satisfactory performance and voltage quality for a DC MG. BESSs also have a constrained lifespan. Therefore, the BESSs lifetime may be shortened by frequent battery charging and discharging due to the instantaneous differences in renewable energy generation or load power fluctuations [10], [11].

A successful combination of Super Capacitors (SCs) and BESSs can effectively address the aforementioned BESS shortcomings [7], [12]. The SCs offer a greater power density and a quicker dynamic response than the BESSs. Therefore, they can release/absorb more energy for a much shorter period of time. They also have a substantially longer lifecycle than BESSs do. Therefore, the repeated charging and discharging of SCs has no impact on their lifespan. However, because to their low energy density, SCs are inappropriate for long-term energy storage applications [13]. Battery-supercapacitor Hybrid Energy Storage Systems (HESSs) combine a BESS and a SC to increase the system's dynamic performance and lengthen its lifespan while taking into account the structural capabilities and limitations of each these BESSs. To do this, the SC absorbs transient power fluctuations from loads (such as PPLs) or renewable resources (such as PV or wind), while the BESS is utilised for steady-state power balancing [10].

The active topologies, which are more desirable due to their better controllability, can be built for HESSs made up of a BESS and SC. Other topologies include passive, semi-active, and active topologies. Aside from the active topologies, the entire dispatch capability of BESS and SC can be used [11]. Each of the HESS components (i.e., the BESS and SC) in these topologies has a separate current control system and is coupled to the MG DC bus via a power electronic converter to offset the higher expense of the active components (such as power electronic converters), a more sophisticated control and Energy Management System (EMS) should be used [14].

The creation of adequate offline and online management and control algorithms is necessary for the HESSs to function effectively and reliably. To determine the appropriate size of the SC, BESS, and other DERs using offline methods, various optimization algorithms (such as stochastic programming or genetic algorithms) can be implemented based on the cost of the system's equipment, the amount of power that the loads are requesting, the availability of renewable energy sources (such as wind or PV), and the size of the SC, BESS, and other DERs. On the other hand, online algorithms are required to guarantee the system's dependable real-time performance. For various objectives, the MG's various control layers can execute real-time management and control procedures. For instance, they can be used in the secondary control layer of the MG for real-time power sharing between the HESS components (i.e., the BESS and SC) and other DERs, or they can be implemented in the tertiary level of the MG for the best (or most economical) State of Charge (SoC) management of the BESSs. To increase the MG's transient voltage stability and voltage quality, they can also be incorporated in the primary control layer for efficient current sharing between the BESS and SC [11].

In DC MG applications, a HESS can function as a grid-forming unit when the DC MG is islanded or as a grid-following unit when the DC MG is connected to the utility grid. In the grid-connected mode of the MG, a bidirectional AC to DC converter is used to connect to the superior AC grid and regulate the DC MG's voltage. Since the HESS is in power (or current) control mode in this instance, its functioning has no effect on the MG's transient voltage stability. In this working mode, the SC absorbs the instantaneous power fluctuations and the EMS (i.e., the tertiary control layer) of the MG computes a reference power for the BESS and SC. In order to achieve efficient power allocation

between the HESS components and reduce the operational cost of the MG, real-time optimization-based energy management solutions can be implemented at the tertiary level of the MG. To achieve this, real-time optimal EMS techniques often take the system's operation over the medium term (i.e., over the course of a few hours), ignoring the system's rapid dynamics connected to primary-level controllers and power electronic converters [11], [15].

The HESS module is in charge of preserving the dynamic stability and voltage quality of the DC MG during grid-forming operation (i.e., the islanded mode of the MG). In this instance, the Proportional-Integral (PI) voltage controller computes a reference current signal, which the HESS receives in order to manage the voltage of the MG DC bus. As a result, the voltage controller and current regulator of the BESS and SC converters, as well as other primary-level controllers, may interface with the HESS power/current allocation system. As a result, the system's voltage quality and transient response may be indirectly impacted by the HESS activities.

Thus, in order to efficiently share the HESS reference current calculated by the MG voltage controller between the SC and BESS, the HESS power/current allocation system should have a substantially faster dynamic reaction than grid-following operation. [7], [16], [17].

The most popular method for MG applications that can be used for grid-following and grid-forming HESS devices is Filtration-Based (FB) power/current allocation. Because FB techniques are computationally simple, they can be used in real-time applications, such as grid-forming HESS units [11], [18]. In this method, the HESS control system divides the HESS reference current/power into high-frequency and low-frequency components using a low-pass or high-pass filter, and then distributes the high-frequency parts to SC and the low-frequency parts to BESS (i.e., operating mode "BESS-SC").

Because SC has a low energy density and a quick charge time (a few seconds, for example), it can be fully charged or discharged right away after a fast change in load. The SoC fluctuation of SC (and its terminal voltage) cannot, however, be automatically constrained by standard FB techniques to a specific range. As a result, they frequently use a rule-based supervisory controller that, if the SoC of SC deviates from a specified range, may disable the filter and transfer the HESS reference current to the BESS (i.e., "BESS-only" operation). In order to keep the SC SoC variation within a predetermined range, the HESS may frequently switch between several operating modes. As a result, the continuous operation of SC is not guaranteed. The voltage quality of MG may be impacted by these switching instances and transient voltage variations that may occur when the system is operating. Additionally, this article looks at the MG voltage control system's marginal stability and compares it to the "BESS-only" operation when a grid-forming HESS operates in the "BESS-SC" mode. Therefore, it is crucial to ensure the ongoing operation of SC due to the destabilising effect of CPLs, especially if the grid-forming HESS is loaded by a significant CPL.

In order to ensure that SC operates continuously, in practise either the size of SC needs to be large enough to handle the significant power/current variations, which raises the initial cost of the system, or the cut-off frequency of the filter needs to be lowered, which shortens the lifetime of the BESS. The previous research of the authors [19] aimed to resolve this problem by creating an active compensating filtering technique that automatically recovers the SoC (or terminal voltage) of SC in order to drastically lower the necessary number of switching instances. To ensure that the SC's SoC variation stays within a predetermined range, that technique still requires a rule-based EMS that can deactivate the SC. A virtual capacitance droop technique that may automatically restore the SoC of SC to a reference value is also suggested in the proposed work in [20]. It is further demonstrated that, provided the droop parameters are properly chosen, this strategy can marginally enhance the marginal stability of MG. One inherent shortcoming of the droop control strategies is that this method may result in a steady-state voltage deviation [21]. Additionally, selecting the proper droop coefficients in DC MGs with numerous loads or DERs might be

a difficult issue.

Model Predictive Control (MPC) techniques have recently attracted a lot of interest in HESS applications. The main principle of MPC is to compute a series of future control actions to minimise a predefined cost function (i.e., optimization step) by using the dynamical model of the system to predict the system's outputs (i.e., prediction step) within a moving horizon (i.e., prediction horizon) [22], [23]. The real-time optimization process of MPC controllers is one of their intriguing aspects. MPC techniques can therefore automatically keep the SoC fluctuation of the HESS components within a given range. However, as compared to rule-based techniques, they have a much larger computational complexity.

The MPC techniques can be used in many control levels for various purposes in DC MGs with HESS technologies. For instance, the references [24]-[28] offer an MPC-based Energy Management System (EMS) for HESSs, in which the MPC controllers are positioned at the tertiary level of the MG and are in charge of scheduling and managing energy usage for various DERs, including the HESS units. The sample time or action time of the MPC controller in these applications is typically in the region of a few minutes. Consequently, the MPC prediction model (i.e., the prediction step) does not take the system's rapid dynamics into account (e.g., primary controllers, power electronic converters, and circuit dynamics). As a result, these techniques don't target the MG's voltage stability or transient responsiveness; instead, they concentrate on enhancing the system's steady state performance. Additionally, the MPC controllers at this layer often have centralised architectures that require knowledge from all DERs to guarantee the efficient operation of MG. As an alternative, the output voltage and currents of the power electronic converters can be controlled using MPC controllers in the primary controller layer of the MG (for example, using direct MPC methods) [22]. For instance, the reference [29] suggests using a Finite Control Set -MPC (FCS-MPC) strategy to increase the grid-forming HESS unit in a DC MG's transient response and resilience. According to this method, the FCS-MPC is positioned at the MG's primary control layer and directly controls the converters' switches to regulate the output current of the BESS and SC to their respective reference values, which are both calculated by an FB power/current allocation system. However, because of their great computational complexity, FCS-MPC techniques could inherently result in unsolvable optimization issues [23]. They also result in variable frequency switching, which affects the output filter design of the converter [30], [31]. Furthermore, their use in DC MG applications necessitates a significant redesign of the inner loop converter controllers, which may not always be possible. The real-time control and management strategies of HESSs are compared in Fig. 1 to the conventional control hierarchy of DC MGs.

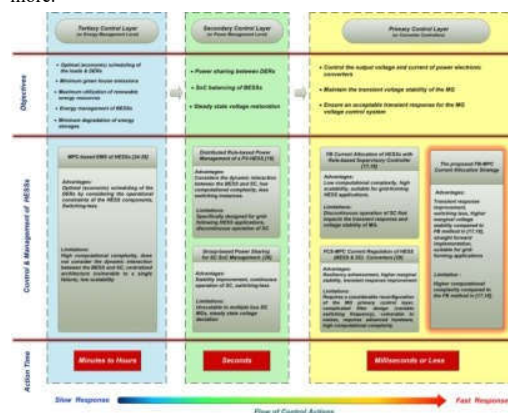
**B. CONTRIBUTION AND SCOPE**

This work makes the following contributions to address the issues raised and enhance the functionality of a grid-forming HESS unit in controlling the MG DC bus voltage (i.e., improving the functionality of the MG primary control layer):

- 1) This study presents a comprehensive state-space dynamic model of an islanded DC MG that receives a CPL from a grid-forming HESS. Furthermore, it is anticipated that the HESS has a standard FB supervisory controller and power/current allocation technique.
- 2) It offers a small-signal stability study to contrast the MG's marginal stability between the HESS's "BESS-SC" and "BESS-only" operating modes. According to the stability analysis, the DC MG exhibits noticeably greater marginal stability when running in the "BESS-SC" mode. This means that the MG PI voltage controller can operate with noticeably higher gain settings and remain stable for longer communication delays if the HESS only executes the "BESS-SC" operating mode.
- 3) The current assignment between the BESS and SC is performed using a Linear Time-Invariant (LTI) filter and an MPC control system using an FB-MPC strategy. In this method, after abrupt load changes, the MPC module immediately recovers the SoC of SC and makes sure that its SoC variation stays within a

predetermined range. As a result, the grid-forming HESS is able to operate continuously in "BESS-SC" mode, ensuring SC's uninterrupted operation. As a result, the PI voltage controller for the MG may function at greater gain levels, improving the voltage quality and transient response, especially when the DC MG is heavily loaded by large CPLs.

4) The proposed MPC controller is different from other MPC strategies used in DC MG applications in that it interacts with the voltage and current regulators of the power electronic converters but is not in charge of controlling their output voltage or current. Instead, it is situated at the primary control layer of the MG. Instead, by computing a compensation term and adding or removing that value from the reference current of the BESS and SC power electronic converters, it is in charge of controlling the SC SoC fluctuation. It is not necessary for it to be as quick as the direct MPC approaches because of this feature (e.g., FCS-MPC). For instance, the direct MPC techniques should have an action time of less than a millisecond, whereas the suggested MPC controller's action time can range from a few milliseconds to more.



**Fig(1):A comparison between different real time control and management strategies of HESSs with respect to the standard hierarchical control structure of DC MGs.**

As a result, this method's optimization stage is simpler (i.e., more suitable for real-time applications). Additionally, neither the power electronic converters nor the dynamics of the MG circuit model are required by its prediction model. Additionally, it does not need details about other DERs, such as their output currents or voltages. Just the filter model, nominal current, and SC charge capacity are needed instead. Because of this, it has a much simpler prediction model. Its decentralised architecture also makes it simple to modify for the multi-generation/multi-bus DC MGs. It should be mentioned that the suggested FB-MPC method seeks to enhance the primary control layer performance of the MG. This work concentrates on the short-term operation of the system (i.e., in the range of a few seconds) to explore the transient response and voltage stability of the system under rapid load changes because the fundamental control layer of MG has very quick dynamic reactions. Therefore, the SoC management of BESSs which often calls for long-term (or mid-term) EMS and power sharing methods and necessitates the right responses from the secondary and tertiary control layers of the MG—is not covered in this work. In terms of the control hierarchy of DC MGs, Fig. 1 contrasts the extent and contribution of this research with that of the reviewed literature. The remainder of this essay is structured as follows: In order to perform a small-signal stability study, Section II builds the dynamical model of the DC MG and outlines the suggested system design. The performance of the MG voltage control system can be negatively impacted by standard FB techniques, which is why using the suggested FB-MPC method may be beneficial. The suggested MPC-based SC SoC restoration technique is then covered in part III. In part IV, computer simulation is used to confirm the effectiveness of the suggested FB-MPC technique. The next directions for research are covered in Section V, and the work is concluded in Section VI.

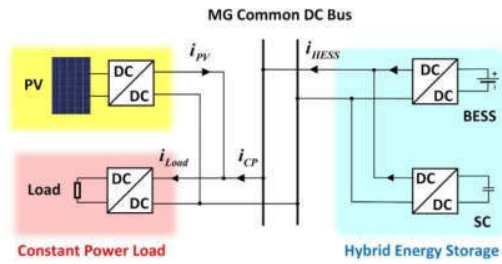


Fig (2): The schematic model of the case study system.

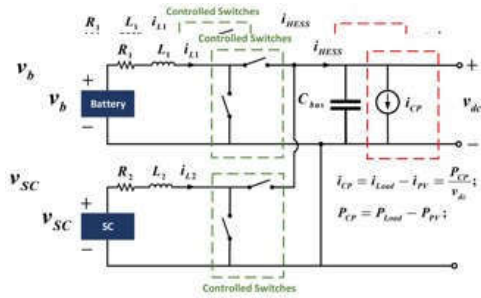


Fig (3): The circuit model of the case study DC MG system.

**II.SYSTEM ANALYSIS:**

The effect of an FB power/current allocation system on the dynamic stability of MG is examined in this section. Figure 2 depicts an islanded DC MG with a PV power production system, a HESS module, and a CPL; the HESS, load, and PV currents are represented, respectively, by  $i_{HESS}$ ,  $i_{Load}$ , and  $i_{PV}$ . The difference between the load and PV currents is also represented by  $i_{CP}$  (i.e.,  $i_{CP} = i_{Load} - i_{PV}$ ). The conventional single bus islanded DC MG suggested in [17], [18], on which the case study system in this work is based, and in which the HESS regulates the common DC bus voltage. As can be seen, a BESS and SC are contained within the HESS module and are both connected in parallel to the MG DC bus by means of bidirectional boost converters. The CPL is regarded as a DC load that is coupled to the MG DC bus via a power electronic converter (also known as a load converter) and requires a constant amount of power under variable MG voltage. Here, it is assumed that the PV is operating as a Constant Power Source (CPS) in Maximum Power Point Tracking (MPPT) mode. Additionally, the HESS functions as a grid-forming device to control the MG DC bus voltage. The equivalent circuit model of the islanded DC MG is shown in Fig. 3, where  $v_b$  and  $v_{SC}$  represent the terminal voltages of the BESS and SC, respectively. The output currents of the BESS and SC are  $i_{L1}$  and  $i_{L2}$ , respectively, while the DC bus voltage is  $v_{dc}$ . PCP is also the difference between the power that the CPL (also known as  $P_{Load}$ ) demands and the power that the CPS generates (i.e.,  $P_{PV}$ ). As a result, the grid-forming HESS module is charged by a CPS when the PV power generation exceeds the power required by the load (i.e.,  $P_{CP} < 0$ ). On the other side, the HESS is loaded by a CPL if the load converter's required power is greater than the PV generation power (i.e.,  $P_{CP} > 0$ ). It is important to note that CPLs negative incremental resistance may reduce the dynamic stability of DC MGs [32], [33]. In order to ensure their dependable functioning, DC MGs that contain big CPLs need a control system with a high marginal stability.

The traditional FB power allocation technique in a grid-forming HESS unit is shown in Fig. 4. In this configuration, the HESS module's reference current, or  $i_{ref}$ , is computed by a Proportional-Integral (PI) controller as part of the voltage regulator, which controls the DC bus voltage. The HESS power allocation module then applies a high-pass filter to the HESS reference current (i.e.,  $i_{ref}$ ) to extract its high frequency components. The HESS current allocation system then performs two modes of operation dubbed "BESS-SC" and "BESS-only" in order to guarantee the secure and

dependable operation of the system. The system allocates the high frequency components of the HESS reference current (i.e.,  $i_{HPF}$ ) to the SC during the "BESS-SC" operating mode (i.e.,  $S = 1$ ) (i.e.,  $i_{SC} = i_{HPF}$ ) (For example,  $i_b, i_{ref}, i_{SC}$ ). On the other side, the supervisory controller may deactivate the filter (or SC) and switch to the "BESS-only" operating mode to avoid SC SoC violation (i.e.,  $S = 0$ ). In this instance, the system assigns the BESS all of the reference current (i.e.,  $i_b, i_{ref}, i_{SC}$ ). Therefore, when the power allocation filter is turned off (i.e., in "BESS-only" mode), the HESS functions like a single BESS. Fig. 5 depicts the condensed logic of the rule-based supervisory controller for SC SoC management. In order to regulate the output currents of the BESS and SC converters to their reference values, i.e.,  $d_1$  and  $d_2$ , the current controllers determine the duty cycle of each working mode. The closed-loop system's state space dynamical model utilising the dynamical model to compares the marginal stability of the DC MG into two different operating modes, namely "BESS-SC" and "BESS-ONLY", by analysing the small-signal stability of the system. It will also go over how the filters time constant (or bandwidth) affects the closed-loop system stability.

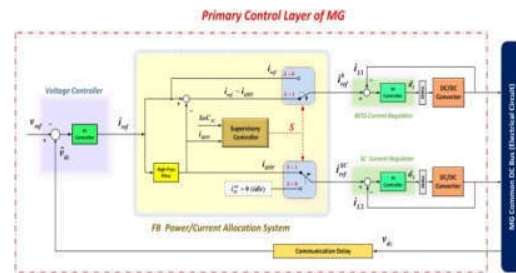
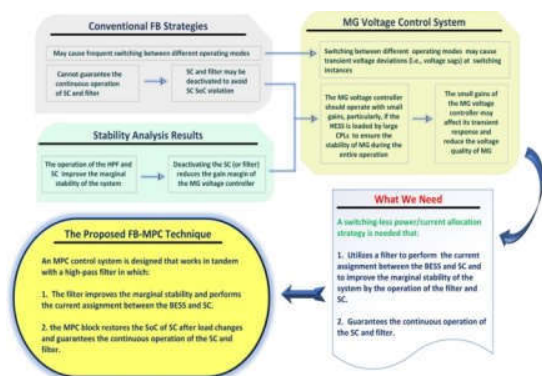


Fig (4): The grid-forming HESS structure with the traditional FB power/current allocation approach from [17], [18].

**III. THE PROPOSED FB-MPC METHOD:**

The proposed FB-MPC approach is displayed in Fig.6. The voltage controller at the MG's primary control layer computes a reference current in this way, which is similar to the FB approach, to manage the common DC bus voltage. The FB-MPC power/current allocation mechanism receives this reference current after that. To ensure the continuous operation of the SC and filter, the suggested technique substitutes an MPC module (see Fig. 4) for the rule-based supervisory controller employed in the traditional FB approach (see Fig. 3). In this method, the MPC module controls the SoC of the SC to a reference value while taking the SoC limitations of the SC into account. In order to accomplish this, the MPC controller uses the discretized dynamical model of the system to forecast the SoC of SC's future error from its reference value over a moving horizon, also known as the prediction horizon. Then, it calculates a series of compensation currents ( $i_{com}$ ) within a moving horizon (i.e., control horizon) and applies the first one to reduce the error. As a result, the MPC compensator transmits a compensation term to the HPF depending on the SoC fluctuation of SC and the HESS reference current (i.e.,  $i_{ref}$ ). The compensating term is added to the reference current of the SC after leaving the HPF and subtracted from the reference current of the BESS after leaving the HPF. As a result, the MPC compensator offers additional BESS and SC coordination so that the BESS gradually charges or releases the SC. As a result, the suggested FB-MPC can regulate the SoC variation within a specified range, ensuring the continued operation of the filter and SC.



Fig(5): Justification of the proposed FB-MPC approach

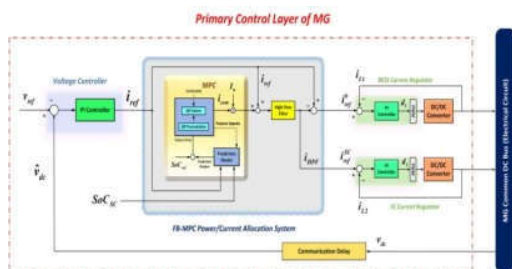


Fig (6): The structure of a grid-forming HESS unit with the proposed FB-MPC power/current allocation system

As can be seen in Fig. 6, the MPC compensator receives the SoC of SC (i.e.,  $SoC_{SC}$ ) and the HESS reference current (i.e.,  $i_{ref}$ ) from the voltage controller in order to regulate the SC SoC variation within a predetermined range. In order to achieve this, the MPC controller uses a dynamic model of the FB current allocation system as well as a dynamic relationship between the SC's current and the SoC value during the prediction stage. In this case, the MPC controller uses the dynamic model of the FB current allocation system to determine how much of the HESS reference current will be assigned to the SC, and then forecasts the SC SoC fluctuation throughout the course of its prediction interval (i.e., the prediction horizon). The MPC will then perform optimization. By taking into account the SC SoC limitations specified in, the controller calculates a series of compensation terms, or  $i_{com}$ , in order to reduce the error between the SC's SoC and its reference value, or  $SoC_{ref}$ . After applying the first value in the sequence, the MPC controller advances to the following time step. Fig. 7 depicts the MPC compensator's flowchart. The HPF is then sent the compensation term.

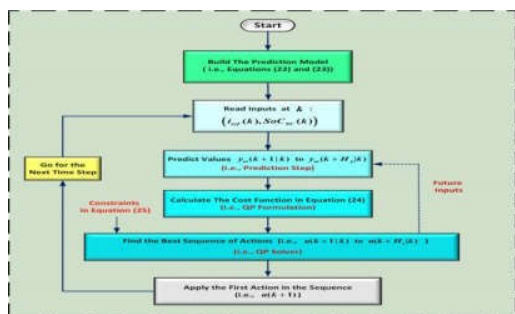


Fig (7): The flowchart of the proposed MPC strategy for SC SoC recovery

The continuous operation of the SC and filter cannot be ensured by the typical FB power/current allocation technique. As a result, the HESS can alternate between the "BESS-only" and "BESS-SC" modes of operation. The MG voltage control system then has

much higher marginal stability in the "BESS-SC" operating mode compared to the "BESS-only" operation, according to the proposed small-signal stability analysis in II.B. As a result, an MPC controller is used to keep the SC's SoC variation within a set range, ensuring the continued operation of the SC and filter. The HESS will therefore always be in the "BESS-SC" operational mode. In order to accomplish this, the MPC controller computes a compensation term ( $i_{com}$ ) and sends it to the HPF (see Fig. 6). As a result, the MPC controller adds the  $d_{com}$  to the SC reference current and subtracts that value from the SC reference current to offer extra coordination between the SC and BESS. Practically speaking, the MPC action time (or MPC sampling time) is substantially longer than the MG voltage controller since the dynamics of the SC SoC change are significantly slower than those of the DC bus voltage. In the MPC cost function, the variation of the MPC compensation current (i.e., the moved variable) is also constrained. The compensation term (i.e.,  $d_{com}$ ) is consequently viewed from the perspective of the MG voltage controller as a minor disturbance with very slow fluctuations. As a result,  $d_{com}$  does not alter the dynamic model of the MG voltage control system (such as the closed-loop poles of the linearized model). Practically speaking, the MPC action time (or MPC sampling time) is substantially longer than the MG voltage controller since the dynamics of the SC SoC change are significantly slower than those of the DC bus voltage.

IV. SIMULATION RESULTS:

The dynamical behaviour of Case 1 (FB) and Case 2 (FB-MPC) systems is evaluated in three separate rapid load (or  $P_{CP}$ ) variation situations in order to assess the effectiveness of the FB-MPC method and compare it with traditional FB power allocation strategies. In the first scenario, the  $P_{CP}$  is abruptly increased from 10 to 15 kW at time  $t = 10$  s, and then abruptly decreased from 15 to 10 kW at time  $t = 25$  s. The DC MG undergoes a quick and periodic pulsed-shape change in  $P_{CP}$  in the second scenario. In the final scenario,  $P_{CP}$  rapidly rises from 10kW to 19kW at  $t = 70$ s before dropping back to 10kW at  $t = 90$ s. The  $P_{CP}$  profile in these three load conditions is shown in Fig. 8. It ought to be It should be emphasised that in reality, the first and third load change scenarios could occur when a load or source converter is added or removed, while the second load change scenario is brought on by the PPLs (such as electric propulsion or laser weapons) inside the DC MG.

During the discussed load change situations, the output power of the BESS and SC in Case 1 (i.e., FB) and Case 2 (i.e., FB-MPC) systems is shown in Fig. 9.  $P_{SC} > 0$  indicates that the SC is discharging, while  $P_{SC} < 0$  indicates that the SC is charging. In both the FB and FB-MPC approaches, the output power of the BESS is smoothed, and the high frequency changes of the  $P_{CP}$  are assigned to the SC, as shown in Fig. 9(a) and (b). Additionally, in both scenarios, the HESS output power (i.e.,  $P_{HESS} = P_b + P_{SC}$ ) is equal to the  $P_{CP}$  (i.e.,  $P_{HESS} = P_{CP}$ ), indicating that power generation and load are in balance. Due to the influence of the MPC compensator, the BESS and SC have slightly different output power profiles in the FB-MPC method compared to the FB approach.

As can be observed in Fig. 11(a), the MPC compensator adds another level of coordination between the BESS and SC in the FB-MPC approach by allowing the BESS to progressively charge and discharge the SC while controlling its SoC variation within a predetermined range. A large quantity of power is supplied to the SC in the third load change scenario (see Figs. 8 and 9) as a result of the severe  $P_{CP}$  variations. As a result, according to the FB approach, the SoC of SC achieves its lowest permitted value at  $t = 73.1$ s (see Fig. 11(a)). In order to operate the BESS solely, the rule-based supervisory controller deactivates the SC and distributes  $P_{HESS}$  power to the BESS. At  $t = 90$  s, the load power abruptly drops, causing the HPF output to turn negative ( $i_{HPF} < 0$ ).

As a result, the rule-based supervisory controller activates the SC and the HESS returns to working in the "BESS-SC" mode.

The SoC of SC, on the other hand, roughly reaches its minimum value at  $t = 74.3s$  in Case 2 (i.e., FB-MPC), as a result of the abrupt change in load at  $t = 70s$ . The MPC parts in Case 1 (FB) and Case 2 (FB-MPC) systems are currently available. As can be observed, the HPF allocates the SC the reference current's high frequency components (i.e., abrupt fluctuations) in order to smooth out the BESS reference current. Additionally, it can be seen that the SC in both scenarios entirely absorbs the high frequency pulsed-shape load changes (i.e., Case 1 and Case 2). As previously mentioned, the SC (or filter) is disengaged at  $t = 73s$  in the third load scenario.

The suggested FB-MPC technique (Case 2) and the standard FB (Case 1) are compared in Fig. 12, where Fig. 12(b) shows the output currents of the HESS components in the Case 1 (FB) and Case 2 (FB-MPC) systems and Fig. 12(a) displays HESS reference currents determined using MG voltage controllers. As can be observed, the HPF allocates the SC the reference current's high frequency components (i.e., abrupt fluctuations) in order to smooth out the BESS reference current. Additionally, it can be seen that the SC in both scenarios entirely absorbs the high frequency pulsed-shape load changes (i.e., Case 1 and Case 2).

As previously established, in the third load scenario, the SC in order to prevent a SC SoC violation, is turned off at  $t = 73.1s$  in Case 1 and the HESS switches to the "BESS-only" operation. The SC current is quickly switched to zero as a result, which can lead to a significant transient voltage sag. However, by including a compensating current, the suggested FB-MPC approach ensures the uninterrupted operation of SC during the full system operation adding that amount to the SC and deducting it from the BESS reference current.

As seen in Fig. 13, when the SoC of SC hits its minimal value at  $t = 74.3s$ , the  $d_{com}$  moves relatively quickly. The MPC forecasts that its output constraint (i.e., the SC SoC allowed range) will be broken at  $t = 73.1s$ .

The BESS and SC terminal voltages during the simulation interval are shown in Fig. 14. As can be observed, the terminal voltage of the BESS (i.e.,  $v_b$ ) stays largely consistent during the simulation session despite the BESS having a substantially longer charge time (i.e., 2 hours). It is also important to note that the suggested FB-MPC strategy results in a different terminal voltage of the SC in Case 2 compared to Case 1 due to a distinct SoC variation caused by the FB method (i.e.,  $v_{sc}$ ). As a result, during system operation, the reference currents of the HESSs in Cases 1 and 2 estimated by the MG voltage controller have somewhat distinct profiles.

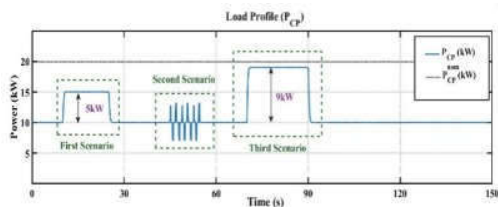


Fig (8). The load change scenarios in the test systems

The dynamical behaviour of Case 1 (FB) and Case 2 (FB-MPC) systems is evaluated in three separate rapid load (or  $P_{CP}$ ) variation situations in order to assess the effectiveness of the FB-MPC method and compare it with traditional FB power allocation strategies. In the first scenario, the  $P_{CP}$  is abruptly increased from 10 to 15 kW at time  $t = 10s$ , and then abruptly decreased from 15 to 10 kW at time  $t = 25s$ . The DC MG undergoes a quick and

periodic pulsed-shape change in PCP in the second scenario. In the final scenario, PCP rapidly rises from 10kW to 19kW at  $t = 70s$  before dropping back to 10kW at  $t = 90s$ . The  $P_{CP}$  profile in these three load conditions is shown in Fig. 8. It ought to be It should be emphasised that in reality, the first and third load change scenarios could occur when a load or source converter is added or removed, while the second load change scenario is brought on by the PPLs (such as electric propulsion or laser weapons) inside the DC MG.

During the discussed load change situations, the output power of the BESS and SC in Case 1 (i.e., FB) and Case 2 (i.e., FB-MPC) systems is shown in Fig. 9.  $P_{SC} > 0$  indicates that the SC is discharging, while  $P_{SC} < 0$  indicates that the SC is charging. In both the FB and FB-MPC approaches, the output power of the BESS is smoothed, and the high frequency changes of the  $P_{CP}$  are assigned to the SC, as shown in Fig. 9(a) and (b). Additionally, in both scenarios, the HESS output power (i.e.,  $P_{HESS} = P_b + P_{SC}$ ) is equal to the PCP (i.e.,  $P_{HESS} = P_{CP}$ ), indicating that power generation and load are in balance. Due to the influence of the MPC compensator, the BESS and SC have slightly different output power profiles in the FB-MPC method compared to the FB approach.

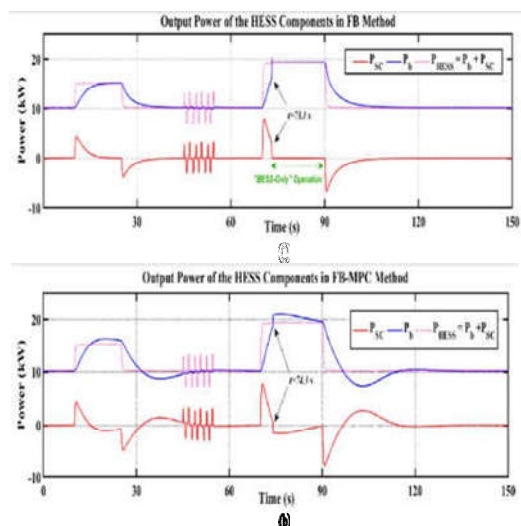


Fig (9). The output power of the HESS components in the test (a) Case 1 (i.e., conventional FB), (b) Case 2 (i.e., the proposed FB-MPC).

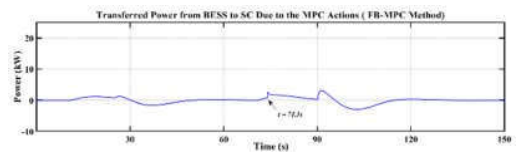


Fig (10). Transferred power from BESS to SC because of the MPC actions in the FB-MPC method.

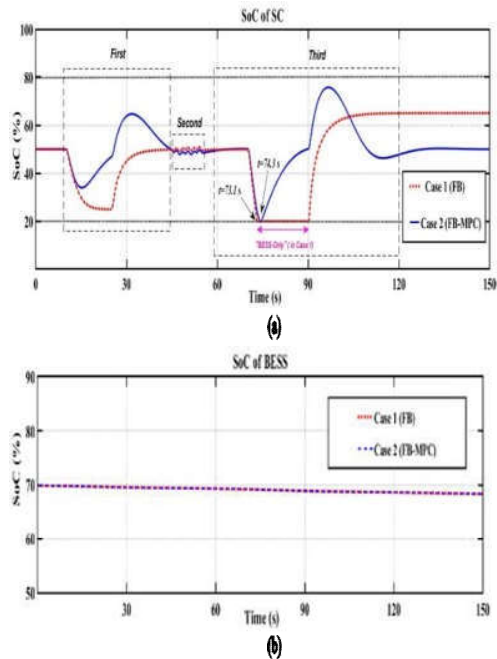


Fig (11). The SC and BESS SoC variation (a) SoC of SC, (b) SoC of BESS

As can be observed in Fig. 11(a), the MPC compensator adds another level of coordination between the BESS and SC in the FB-MPC approach by allowing the BESS to progressively charge and discharge the SC while controlling its SoC variation within a predetermined range. A large quantity of power is supplied to the SC in the third load change scenario (see Figs. 13 and 14) as a result of the severe PCP variations. As a result, according to the FB approach, the SoC of SC achieves its lowest permitted value at  $t = 73.1s$  (see Fig. 11(a)). In order to operate the BESS solely, the rule-based supervisory controller deactivates the SC and distributes PHESS power to the BESS. At  $t = 90s$ , the load power abruptly drops, causing the HPF output to turn negative ( $i_{HPF} < 0$ ). As a result, the rule-based supervisory controller activates the SC and the HESS returns to working in the "BESS-SC" mode.

The SoC of SC, on the other hand, roughly reaches its minimum value at  $t = 74.3s$  in Case 2 (i.e., FB-MPC), as a result of the abrupt change in load at  $t = 70s$ . The MPC parts in Case 1 (FB) and Case 2 (FB-MPC) systems are currently available. As can be observed, the HPF allocates the SC the reference current's high frequency components (i.e., abrupt fluctuations) in order to smooth out the BESS reference current. Additionally, it can be seen that the SC in both scenarios entirely absorbs the high frequency pulsed-shape load changes (i.e., Case 1 and Case 2). As previously mentioned, the SC (or filter) is disengaged at  $t = 73s$  in the third load scenario.

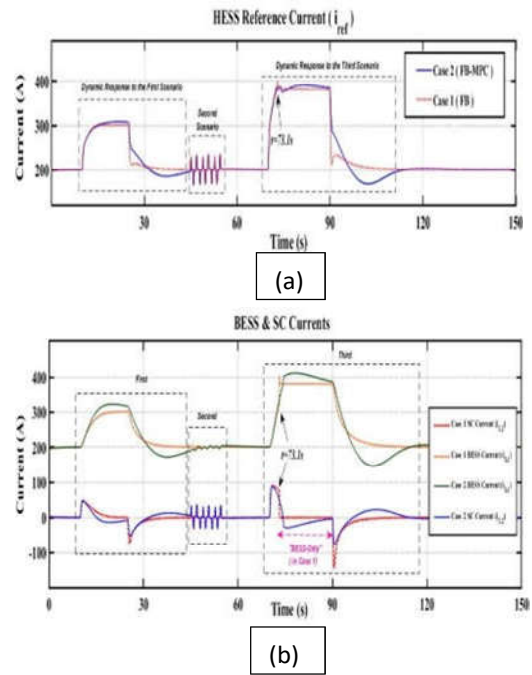


Fig (12). The performance of the current allocation systems in the case study MGs (i.e., Case1 and Case 2). (a) HESS reference current (b) The SC and BESS currents.

The suggested FB-MPC technique (Case 2) and the standard FB (Case 1) are compared in Fig. 12, where Fig. 12(b) shows the output currents of the HESS components in the Case 1 (FB) and Case 2 (FB-MPC) systems and Fig. 12(a) displays HESS reference currents determined using MG voltage controllers. As can be observed, the HPF allocates the SC the reference current's high frequency components (i.e., abrupt fluctuations) in order to smooth out the BESS reference current. Additionally, it can be seen that the SC in both scenarios entirely absorbs the high frequency pulsed-shape load changes (i.e., Case 1 and Case 2).

As previously established, in the third load scenario, the SC in order to prevent a SC SoC violation, is turned off at  $t = 73.1s$  in Case 1 and the HESS switches to the "BESS-only" operation. The SC current is quickly switched to zero, which can lead to a significant transient voltage sag. However, by including a compensating current, the suggested FB-MPC approach ensures the uninterrupted operation of SC during the full system operation adding that amount to the SC and deducting it from the BESS reference current.

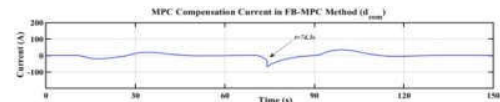
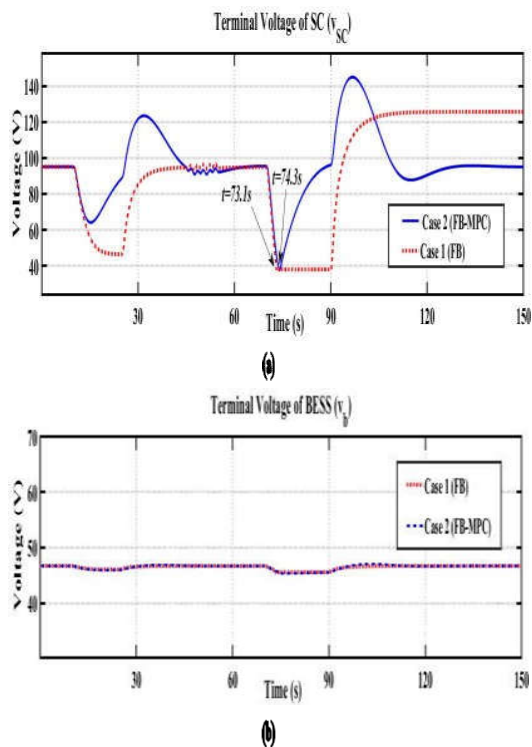


FIGURE 13. The MG DC bus voltage during the load change scenarios.

As seen in Fig. 13, when the SoC of SC hits its minimal value at  $t = 74.3s$ , the  $d_{com}$  moves relatively quickly. The MPC forecasts that its output constraint (i.e., the SC SoC allowed range) will be broken at  $t = 73.1s$ .



**Fig (14).** The output power of the HESS components in the test cases (a) Case1 (i.e., conventional FB), (b) Case 2 (i.e., the proposed FB-MPC).

The BESS and SC terminal voltages during the simulation interval are shown in Fig. 14. As can be observed, the terminal voltage of the BESS (i.e.,  $v_b$ ) stays largely consistent during the simulation session despite the BESS having a substantially longer charge time (i.e., 2 hours). It is also important to note that the suggested FB-MPC strategy results in a different terminal voltage of the SC in Case 2 compared to Case 1 due to a distinct SoC variation caused by the FB method (i.e.,  $v_{sc}$ ). As a result, during system operation, the reference currents of the HESSs in Cases 1 and 2 estimated by the MG voltage controller have somewhat distinct profiles.

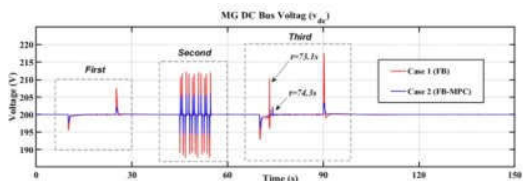


**Fig (15).** The MG DC bus voltage during the load change scenarios.

**CONCLUSION**

FB techniques are widely used in HESS applications to achieve the power/current allocation between the BESS and SC. An LTI filter is frequently used to separate the high and low-frequency components of the HESS reference power/current, with the high-frequency components then being assigned to SC. This paper initially presents a small-signal stability analysis to ascertain the impacts of the HESS current assignment filter on the dynamic stability of a single bus DC MG in which a grid-forming HESS supplies a CPL. The stability analysis demonstrates that the present assignment filter improves the marginal stability of the

MG. The MG PI voltage controller can work at higher gain settings and withstand longer communication delays thanks to the continuous operation of the SC and filter. The SC and filter cannot, however, work continuously under rapid load fluctuations when employing the typical FB techniques. In order to develop an MPC-based SC SoC restoration solution that addresses this problem, the current allocation between the BESS and SC is carried out in this research together with an LTI filter. In this system, the SC and filter are guaranteed to operate continuously since the MPC controller maintains the SoC of the SC within a set range. As a result, the suggested method indirectly enhances the system's transient response and voltage quality by allowing the MG voltage controller to operate at greater gain levels. After that, a case study DC MG simulation in MATLAB/Simulink is used to confirm the effectiveness of the suggested FB-MPC approach.

**REFERENCES**

- [1] M. Fotuhi Firuzabad, R. Iravani, F. Aminifar, N. Hatziargyriou, and M. Lehtonen, "Guest editorial special section on microgrids," *IEEE Trans. Smart Grid*, vol. 3, no. 4, pp. 1857–1859, Dec. 2012.
- [2] M. Ahmed, L. Meegahapola, A. Vahidnia, and M. Datta, "Stability and control aspects of microgrid architectures—A comprehensive review," *IEEE Access*, vol. 8, pp. 144730–144766, 2020.
- [3] L. Meng, Q. Shafiee, G. F. Trecate, H. Karimi, D. Fulwani, X. Lu, and J. M. Guerrero, "Review on control of DC microgrids and multiple microgrid clusters," *IEEE J. Emerg. Sel. Topics Power Electron.*, vol. 5, no. 3, pp. 928–948, Sep. 2017.
- [4] M. K. Al-Nussairi, R. Bayindir, S. Padmanaban, L. Mihet-Popa, and P. Siano, "Constant power loads (CPL) with microgrids: Problem definition, stability analysis and compensation techniques," *Energies*, vol. 10, no. 10, p. 1656, Oct. 2017.
- [5] O. Lorzadeh, I. Lorzadeh, M. N. Soltani, and A. Hajizadeh, "Source-side virtual RC damper-based stabilization technique for cascaded systems in DC microgrids," *IEEE Trans. Energy Convers.*, vol. 36, no. 3, pp. 1883–1895, Sep. 2021.
- [6] M. Hassan, M. Worku, A. Eladl, and M. Abido, "Dynamic stability performance of autonomous microgrid involving high penetration level of constant power loads," *Mathematics*, vol. 9, no. 9, p. 922, Apr. 2021.
- [7] Q. Xu, N. Vafamand, L. Chen, T. Dragicevic, L. Xie, and F. Blaabjerg, "Review on advanced control technologies for bidirectional DC/DC converters in DC microgrids," *IEEE J. Emerg. Sel. Topics Power Electron.*, vol. 9, no. 2, pp. 1205–1221, Apr. 2021.
- [8] Y. Wang, L. Wang, M. Li, and Z. Chen, "A review of key issues for control and management in battery and ultracapacitor hybrid energy storage systems," *eTransportation*, vol. 4, May 2020, Art. no. 100064.
- [9] A. A. K. Arani, G. B. Gharehpetian, and M. Abedi, "Review on energy storage systems control methods in microgrids," *Int. J. Electr. Power Energy Syst.*, vol. 107, pp. 745–757, May 2019.
- [10] M. E. Şahin and F. Blaabjerg, "A hybrid PV-battery/supercapacitor system and a basic active power control proposal in MATLAB/Simulink," *Electronics*, vol. 9, no. 1, p. 129, Jan. 2020.
- [11] S. Hajjaghasi, A. Salemnia, and M. Hamzeh, "Hybrid energy storage system for microgrids applications: A review," *J. Energy Storage*, vol. 21, pp. 543–570, Feb. 2019.
- [12] N. R. Tummuru, U. Manandhar, A. Ukil, H. B. Gooi, S. K. Kollimala, and S. Naidu, "Control strategy for AC-DC microgrid with hybrid energy storage under different



- operating modes," *Int. J. Electr. Power Energy Syst.*, vol.104, pp. 807–816, Jan.2019.
- [13] V. T. Nguyen and J. W. Shim, "Virtual capacity of hybrid energy storage systems using adaptive state of charge range control for smoothing renewable intermittency," *IEEE Access*, vol. 8, pp. 126951–126964, 2020.
- [14] W. Jing, C. H. Lai, W. S. H. Wong, and M. L. D. Wong, "Dynamic power allocation of battery-supercapacitor hybrid energy storage for standalone PV microgrid applications," *Sustain. Energy Technol. Assessments*, vol. 22, pp. 55–64, Aug. 2017.
- [15] X. Lu, Y. Chen, M. Fu, and H. Wang, "Multi-objective optimization- based real-time control strategy for battery/ultracapacitor hybrid energy management systems," *IEEE Access*, vol. 7, pp. 11640–11650, 2019.
- [16] X. Chang, Y. Li, X. Li, and X. Chen, "An active damping method based on a supercapacitor energy storage system to overcome the destabilizing effect of instantaneous constant power loads in DC microgrids," *IEEE Trans. Energy Convers.*, vol. 32, no. 1, pp. 36–47, Mar.2017.
- [17] S. Kotra and M. K. Mishra, "Design and stability analysis of DC microgrid with hybrid energy storage system," *IEEE Trans. Sustain. Energy*, vol.10, no. 3, pp. 1603–1612, Jul.2019.
- [18] P. Singh and J. S. Lather, "Power management and control of a grid- independent DC microgrid with hybrid energy storage system," *Sustain. Energy Technol. Assessments*, vol. 43, Feb. 2021, Art. no.100924.
- [19] S. A. G. K. Abadi and A. Bidram, "A distributed rule- based power management strategy in a photovoltaic/hybrid energy storage based on an active compensation filtering technique," *IET Renew. Power Gener.*, vol. 15, no. 15, pp. 3688–3703, Nov.2021.
- [20] Q. Xu, X. Hu, P. Wang, J. Xiao, P. Tu, C. Wen, and M. Y. Lee, "Decentralized dynamic power sharing strategy for hybrid energy storage system in autonomous DC microgrid," *IEEE Trans. Ind. Electron.*, vol.64, no. 7, pp. 5930–5941, Jul.2017.
- [21] U. B. Tayab, M. A. Roslan, L. J. Hwai, and M. Kashif, "A review of droop control techniques for microgrid," *Renew. Sustain. Energy Rev.*, vol. 76, pp. 717–727, Sep. 2017.
- [22] J. Hu, Y. Shan, J. M. Guerrero, A. Ioinovici, K. W. Chan, and J. Rodriguez "Model predictive control of microgrids—An overview," *Renew. Sust. Energ. Rev.*, vol.136, Feb. 2021, Art. no.110422.
- [23] P. Karamanakos, E. Liegmann, T. Geyer, and R. Kennel, "Model predictive control of power electronic systems: Methods, results, and challenges," *IEEE Open J. Ind. Appl.*, vol. 1, pp. 95–114, 2020.
- [24] U. R. Nair and R. Costa-Castello, "A model predictive control-based energy management scheme for hybrid storage system in islanded microgrids," *IEEE Access*, vol. 8, pp. 97809–97822, 2020.
- [25] X. Zhang, B. Wang, D. Gamage, and A. Ukil, "Model predictive and iterative learning control-based hybrid control method for hybrid energy storage system," *IEEE Trans. Sustain. Energy*, vol. 12, no. 4, pp. 2146–2158, Oct. 2021.
- [26] H. Chen, R. Xiong, C. Lin, and W. Shen, "Model predictive control based real-time energy management for hybrid energy storage system," *CSEE J. Power Energy Syst.*, vol. 7, no. 4, pp. 862–874, Jul. 2021.
- [27] Z. Jia, J. Jiang, H. Lin, and L. Cheng, "A real-time MPC-based energy management of hybrid energy storage system in urban rail vehicles," *Energy Proc.*, vol. 152, pp. 526–531, Oct.2018.
- [28] F. Garcia-Torres, L. Valverde, and C. Bordons, "Optimal load sharing of hydrogen-based microgrids with hybrid storage using model-predictive control," *IEEE Trans. Ind. Electron.*, vol. 63, no. 8, pp. 4919–4928, Aug. 2016.